IEEE Access
Multidisciplinary | Rapid Review | Open Access Journal

Received August 6, 2019, accepted September 5, 2019, date of publication September 11, 2019,
date of current version September 23, 2019.

Digital Object Identifier 10.1109/ACCESS.2019.2940236

Research on the Dynamic Characteristics in the Flocculation Process of Mineral Processing Tailings

RUGAO GAO[1,2], (Member, IEEE), KEPING ZHOU[1,2], JIAN ZHANG[1,2], (Member, IEEE), HONGQUAN GUO[1,2], AND QIFAN REN[1]

[1]School of Resources and Safety Engineering, Central South University, Changsha 410083, China
[2]Research Center for Mining Engineering and Technology in Cold Regions, Central South University, Changsha 410083, China

Corresponding authors: Jian Zhang (zhangj@csu.edu.cn) and Hongquan Guo (guohongquan@csu.edu.cn)

This work was supported by the National Natural Science Foundation of China under Grant 51774323.

ABSTRACT Abandoned mineral management has become an important global issue, and the collection, recycling, and disposal of mineral processing tailings (MPT) is critical in both mining engineering and environmental protection. In this study, flocculation sedimentation experiments and slurry rheological tests were carried out with unclassified tailings, and the flocculation sedimentation behaviour of the tailings under different conditions was investigated. The experimental results showed the followings: (1) Under close sedimentation effect conditions, different flocculants showed different effects on the fluidity of the slurry underflow, which was used as an important basis for optimization of the flocculation effect. (2) A tailings solid mass concentration of 40% and a flocculant dosage of 25 g/t were obtained as preferable sedimentation conditions. (3) Based on a microparticle agglomeration characteristics tests at the initial stage of flocculation, a flocculation concentration kinetic model was established that conformed to the fractal characteristics of the particles, which improved the applicability and accuracy of the concentration kinetic equation and the characteristic variables. In this study, an objective method for determining the parameters of full tailings flocculation sedimentation was realized. The results of an industrial trial operation also verified the reliability of the preferred parameters, which provided an effective basis for refined control of an efficient tailings recycling process.

INDEX TERMS Mineral processing tailings, flocculation sedimentation process, rheological characteristics, particle agglomeration.

I. INTRODUCTION

At present, beneficiation is gradually becoming more complicated as ore grades decrease, resulting in a finer grain size of MPT (mineral processing tailings) and an increased output [1]–[3]. Currently, the main tailings disposal methods are surface storage and underground backfilling. More than 25 billion tons of MPT have been produced in China, resulting in approximately 12,000 tailings dams. Similar statistics illustrating the poor disposal of MPT can be observed in Australia, Brazil, America, and Canada [4], [5]. Tailings slurries of low concentrations have a large, immobilized water content, and generate large amounts of overflow when piled up or filled. This situation will not only cause instability of the accumulation body but also easily lead to a series of problems such as environmental pollution and engineering disaster. It is necessary to treat the tailings slurry using flocculation sedimentation technology. The promotion of MPT flocculation sedimentation technology will not only aid in environmental protection but also enable concentrated tailings to be used for mine backfilling, which has significant economic benefits [6]–[8].

With the increase in environmental protection requirements for mines, deep-cone thickeners have been widely studied. The working principle of deep-cone thickeners is adding various flocculant solutions to MPT slurries with lower contents. Through the bridging effect of the flocculant, the MPT particles are gradually enriched to form large flocs.

The associate editor coordinating the review of this manuscript and approving it for publication was Jenny Mahoney.

Finally, the flocs move to the bottom of the thickener, and dewatered to form a high content slurry [9]. The efficiency and effectiveness of the deep-cone thickener mainly depend on three aspects: the flocculation effect, bed compression, and truss operation. These three aspects are directly related to the particle size and structure and the surface chemical properties of the flocs. The formation of the flocs also determines the rheological characteristics of the slurry.

Some studies have been carried out on factors such as the type of flocculant, the sedimentation time, and the consumption of the flocculant [10]–[12], and the sedimentation velocity and bottom flow volume fraction are taken as evaluation indicators in these studies. In fact, the residence time of the slurry and the bottom flow volume fraction are limited by the compaction dewatering process, and the flocculation effect cannot be fully described by the sedimentation velocity and bottom flow volume fraction. This single-factor optimization approach may result in low flocculation efficiency or crushing accidents. With thickeners, the yield stress of the slurry can measure the stability of a truss operation and the damaging effect on a floc network structure. In addition, slurries with low viscosity have good dehydration performance. The rheological properties of the slurry can be used as important indicators reflecting the flocculation effect of the MPT. The sedimentation of the MPT is a rapid process. The tailing particles form a large floc through the bridging effect of the flocculant, which changes the surface area of the particles and the distribution of immobilized water [13]. This effect reduces the concentration of water, and improves the dewatering capacity of the tailings [14]. The reorganization of the floc structure is closely related to the sedimentation parameters.

The macroscopic static sedimentation process is analysed in most current studies, but consideration of the rheological properties and agglomeration characteristics of the MPT slurry is insufficient. Most MPTs used in sedimentation experiments are generally classified tailings that are not fine or muddy or are unclassified tailings with less-fine particles. The single object control method is also a common method used in these experiments [15], [16]. In fact, flocculation is a complex process. The sedimentation velocity and concentration of the particles are affected by factors such as the surface charge properties, particle size, feed concentration, flocculant type, and unit consumption [17]. Therefore, it is important to investigate the internal laws of flocculation through accurate experiments [18], [19].

This research was aimed to offer a new approach for optimizing the flocculation sedimentation parameters of MPT. The sedimentation behaviour of MPT with the use of different flocculant functions and consumption parameters was analysed through indoor flocculation sedimentation experiments. The actual production quality under different flocculation conditions was analysed by underflow rheological shear tests. A floc formation test in the initial stage of flocculation was carried out based on the results of preliminary experiments, and the behavioural equations corresponding to the flocculation kinetic model were established. The flocculation kinetic behaviour of the MPT slurry was analysed from a microscopic perspective. Industrial parameters optimized by this new approach can ensure high-quality underflow production and achieve an efficient and stable flocculation process.

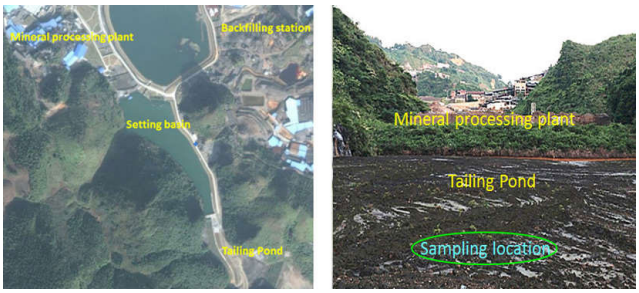

FIGURE 1. MPT sampling.

II. MATERIALS AND METHODS

A. MATERIALS

1) MPT SAMPLING

In this study, the MPT of the Gaofeng Mine in Guangxi Province of China was used for the flocculation experiments. The main minerals processed by the Gaofeng mine are tin sulfide ore and some associated lead-zinc ore. Flotation is the main method of mineral processing. The use of MPT for backfilling not only maintains the stability of the underground construction but also reduces the cost and environmental pressure caused by the expansion of the tailings pond. Therefore, solving the problem of flocculation and the sedimentation of MPT is the key for sustainable mining. The tailings are discharged into a tailings pond after the beneficiation process, and the sewage is recycled after purification treatment in the setting basin (Figure 1). MPT used in this study were sampled at the tailings pond near the plant, transported to the laboratory, and dried by a BGZ-146 Electro-thermostatic blast oven to avoid the loss of fine particles. MPT samples are viscous and must be uniformly mixed before the test to maintain the original particle size characteristics.

2) FLOCCULANTS AND WATER

Several flocculants commonly used in industrial production were selected for the MPT flocculation sedimentation test. These four flocculants were selected for the sedimentation experiments: (1) Germany BASF low-molecular-weight flocculant (an inorganic low-molecular-weight compound, such as $FeSO_4 \cdot 7H_2O$), (2) BASF high-molecular-weight cationic flocculant (the main component of the agent is a polyacrylamide), (3) Northern chemical cationic flocculant (the main component of the agent is a polyacrylamide), and (4) French Eisen 655S flocculant (the main component of the agent is an anionic acrylamide polymer). The water used in the leaching experiment was groundwater collected from the mine inflow of the Gaofeng Mine, which was sealed in plastic buckets prior to further analysis. The pH of the test water was 7.45,

TABLE 1. Ionic components of the water.

Ion type	Ca^{2+}	Mg^{2+}	$Na^{+}+K^{+}$	Cl^{-}	SO_4^{2-}	$CO_3^{2-}+HCO_3^{-}$
Content (mg/L)	30.20	2.39	5.38	8.96	9.06	50.01

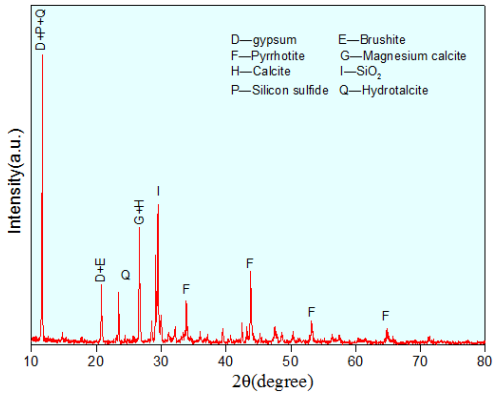

FIGURE 2. XRD profile of the MPT.

the COD value was 15.04, and the content of harmful substances was low. The main ionic components in the water used in this test are presented in Table 1.

B. EXPERIMENTAL METHODS

1) PHYSICAL-CHEMICAL TESTING

The volumetric flask method was used for determining the specific gravity of the sample. The total weight was measured after the dried tailings were added with water and stirred uniformly. The bulk density was determined by the constant volume weighing method. The tailings were freely and slowly dropped into the standard container until they were filled; then, the weight of the container was measured. The angle between the natural slope and the horizontal plane in the loose state of the tailings was measured to obtain the natural repose angle of the MPT. The specific gravity, bulk density, porosity, and natural repose angle measurement results for the sample are presented in Table 2. The mineral composition of the tailings is shown in Figure 2 determined using X-ray diffraction. Table 3 summarizes the chemical compositions of the MPT. The compositional content has an effect on the properties of the backfill material. In the MPT samples tested, the main components were silica (41.59%) and calcium oxide (18.94%) with a small amount of iron and sulfur. The key product in the formation of the backfill was hydrated calcium silicate. Based on the chemical composition analysis, this type of MPT can be combined with pore water in the backfill hydration process.

2) PARTICLE SIZE MEASUREMENT

The difference in particle size and particle composition results in different material properties. Particle size and distribution characteristics are indicators for evaluating various properties of materials and for characterizing the ultimate solids content and rheological properties of materials to satisfy transport conditions. It is recognized that the solid content of particles smaller than 20 μm must be above 25% (weight ratio) to form a stable paste material suitable for pipeline transportation [19].

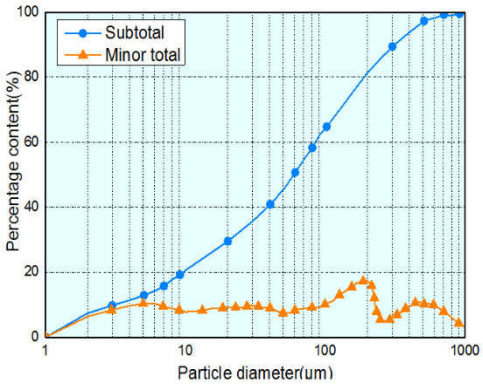

FIGURE 3. Particle size distribution of the MPT.

There are many methods for measuring the particle size of the tailings, and laser particle size testing is currently more accurate than many of the methods. A MASTERSIZER 2000 particle size analyzer was used in this test. The MPT was dried and put into the mixer of the analysis system. This system allows for self-hydration and mixing. The particle size analyser was run continuously until a slurry with a fixed mass fraction formed, and then the particle size of the sample was tested by diffraction.

As shown in Figure 3, The average particle size of the MPT was 110.597 μm. Among the MPT, the content of the ~75 μm particles was 56.69%, and the content of fine particles of ~20 μm was 29.63%. The subtotal particle size distribution results indicate $d_{10} = 3.678$ μm, $d_{50} = 58.599$ μm, and $d_{90} = 304.339$ μm.

The unevenness coefficient is usually used to identify the gradation of the MPT. The unevenness coefficient of the selected sample was $\alpha = d_{60}/d_{10} = 19.91$, which indicates that the particle size distribution is wide, and favourable for compaction [20]. However, the presence of a certain amount of fine mud in the MPT resulted in a small permeability coefficient, which is detrimental to the dehydration and rapid hardening of the backfill. Therefore, it is necessary to select suitable flocculants, unit consumption, and flocculant concentrations to achieve efficient sedimentation.

3) FLOCCULATION SEDIMENTATION EXPERIMENT

The MPT sedimentation experiment is shown in Figure 4. The sedimentation interface observation method was used for this analysis. A transparent glass cylinder with a capacity of 0.5 L was used in this test. To facilitate the determination and calculation of the slurry concentration in the sedimentation test, the slurry was filled to a specified volume of the graduated cylinder, and then the whole scale of the coordinate paper

TABLE 2. Basic physical properties of the tailings.

Materials	Specific gravity (g/cm^3)	Aggregate bulk density (t/m^3)	Compacted density (t/m^3)	Porosity (%)	Natural repose angle (°)
MPT	3.093	1.472	1.789	42.16	34.95

TABLE 3. Chemical composition of the tailings.

Chemical composition	SiO_2	Al_2O_3	CaO	MgO	Fe	Sn
(wt. %)	41.59	2.3	18.94	0.83	5.34	0.27
Chemical composition	Sb	Zn	In	Pb	S	Others
(wt. %)	0.26	1.24	0.0011	0.27	5.79	23.17

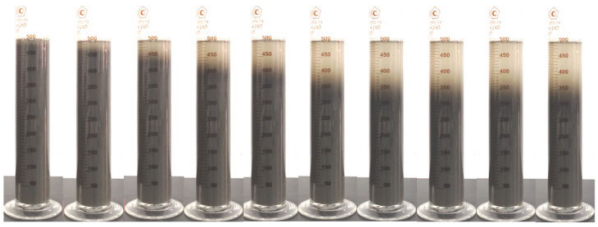

FIGURE 4. Flocculation sedimentation experiment.

was aligned with the scale line of the specified full volume of the measuring cylinder. The scale line is the starting point of the sedimentation, namely, the zero point of sedimentation, and then the sedimentation height was marked successively downward until the bottom of the measuring cylinder. In the measuring cylinder, the MPT slurry should be thoroughly stirred by the agitator. The time is started after the slurry is taken out of the agitator and kept still. The sedimentation height of the material group in the measuring cylinder or the height of the clear water layer is observed, and the sedimentation height of the material group at different sedimentation time points is recorded. Currently, in the industrial production of the Gaofeng mine, the flocculant concentration of the experiment is adjusted to 0.3%, the flocculant dosage was 20 g/t, and the slurry solid mass concentration was 40% by weight. The samples in the experiment were divided into 3 groups of A, B, and C. Groups A, B, and C were tested to analyse the effect of the following factors on the sedimentation characteristics: flocculant type, slurry solid mass concentration, and flocculant dosage. The bottom flow was collected for an indoor rheological shear test after the sedimentation. Some parameters can be visually derived from the sedimentation test, such as net increase in clean water, amount of slurry, total amount of clean water and slurry, slurry concentration after sedimentation, and bulk density.

4) SLURRY RHEOLOGICAL TEST

Sometimes the difference in sedimentation effect caused by flocculants during the test is not obvious. To investigate the effect of flocculation on the quality of the concentrated slurry, the slurry rheological test was performed. Shear rate scanning is a test method that loads a linear or linearly reduced shear rate to the slurry. By using a one-way ascending scanning method, it is possible to examine the rheological properties of materials changing from solid to fluid. The rheological characteristic test can verify the quality of the concentrated underflow and prevent the occurrence of a solidification channel in the slurry. The Huck VT550 rotary rheometer was used to test the rheological properties of the slurry. The test principle was to immerse the four blades in the slurry and rotate at different shear rates. Real-time monitoring was performed by the control software, and the shear stress-shear rate curve output was processed. The wall slip effect was avoided due to yielding near the cylindrical surface created by the rotation of the blade rotor.

5) MICROSCOPIC ANALYSIS

To verify the results of the sedimentation and rheological tests, slurries with different flocculant dosages were added to the particle size analyser, and the particle size data of the first 3 min were collected. In this process, different samples were prepared by taking the floc solution at various stages with a plastic dropper, and image acquisition was performed by using an electron microscopy imaging system. The morphology of the obtained flocs was statistically analysed with image processing software.

III. RESULTS AND DISCUSSION

A. EFFECT OF FLOCCULANT TYPES ON SEDIMENTATION BEHAVIOUR OF MPT

The flocculant currently used in the Gaofeng mine is a BASF high-molecular-weight cationic flocculant. To demonstrate the relationship between the effect of the flocculant and the experimental method, the effects of the four flocculants were observed using the original industrial parameters in Group A. The flocculants used in each scheme of Group A were as follows: (1) Germany BASF low-molecular-weight

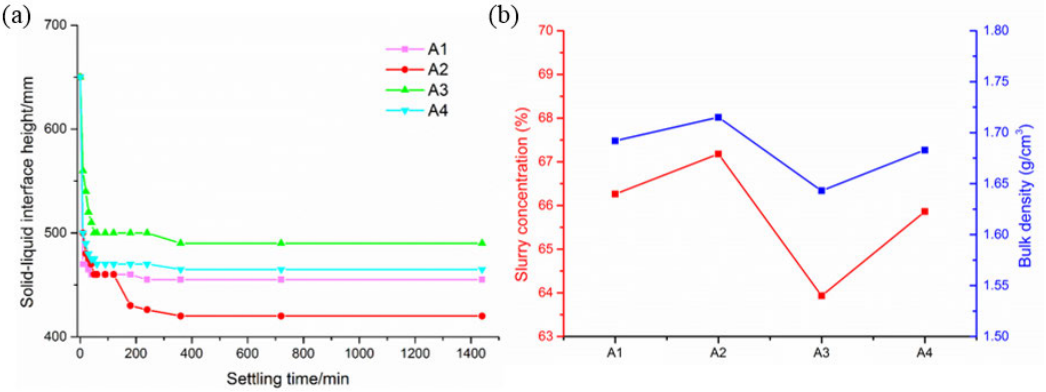

FIGURE 5. Group A sedimentation test results (a) Sedimentation monitoring (b) Sedimentation test parameters.

flocculant, (2) BASF high-molecular-weight cationic flocculant, (3) Northern chemical cationic flocculant, and (4) French Eisen 655S flocculant. During the sedimentation process, the solid-liquid separation interface of each scheme decreased sharply, and then gradually slowed down. There were slight changes in the clear water and bottom flow, but they eventually stabilized. The flocculant was added during the sedimentation process of the tailings. The long chain structure between the flocculant molecules had obvious adsorption of the MPT particles and formed larger agglomerates, which accelerated the sedimentation of the tailings particles. The macroscopic representation of this effect was the liquid surface separation phenomenon in the MPT slurry experiment. Three sub-zones were formed from top to bottom in the graduated cylinder: the clarification zone, the sedimentation zone, and the underflow compression zone. The clarification area continued to expand with extended observation time, and the interface between the clarification zone and the sedimentation zone became obvious. A continuous drop of MPT particles can be observed from the upper part of the sedimentation zone. Continuous deposition occurred in the compression zone, and the fine tailings particles in the supernatant gradually decreased. The results of Group A flocculation sedimentation experiments are shown in Figure 5(a).

It was observed from the flocculation sedimentation test that the main sedimentation process occurred in the first few minutes. After the flocculant was added, the interface between the slurry and water rapidly appeared. Over time, the clarified area became clearer and eventually reached the maximum sedimentation concentration. In the later stage of observation, it was a process of flocculation and compaction, and the interface position was stabilized. The sedimentation test parameters of Group A are shown in Figure 5(b). After the addition of various flocculants, using the same industrial parameters showed that the sedimentation effect of the BASF high-molecular-weight cationic flocculant was slightly better than that of the other flocculants. The flocculants mainly acted at the initial stage of the test, and then the apparent sedimentation characteristics were not obvious, as the flocculation entered the stage of consolidation.

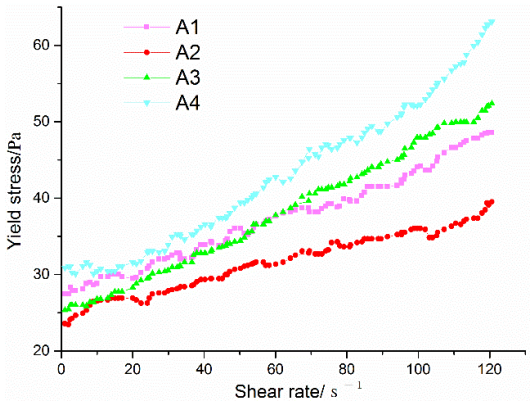

FIGURE 6. Rheological characteristics of the MPT slurry with different flocculants.

In fact, the method of analysing the effects of different flocculants by sedimentation parameters was not particularly significant. After the supernatant was extracted from each sample of Group A, the steady-state rheological characteristics of the concentrated underflow were tested at a uniform shear rate to evaluate the fluidity. According to the shear rate requirement of the MPT slurry, the shear rate range of the test was set to 0-120 s^{-1}, and the apparent viscosity and shear stress of the concentrated underflow at different shear rates were tested. The test results are shown in Figure 6.

It can be seen from the test results that the yield stress of the samples increased linearly with a uniform shear rate. The initial yield stress of the slurry with different flocculants ranged from 23.57 Pa to 30.90 Pa. The initial yield stress is a characterization of the fluidity of the slurry. The consolidation degree of the different samples with approximate concentrations was compared by testing.

It was observed that small flocs were formed under the action of static electricity after the flocculant was added to the MPT slurry. It is known from literature that during the mixing process, the carbon groups and other groups on the flocculant polymer chain interact with the tailings particles through hydrogen bonding forces, van der Waals forces, and ionic bond forces. The floc structure formed under the action

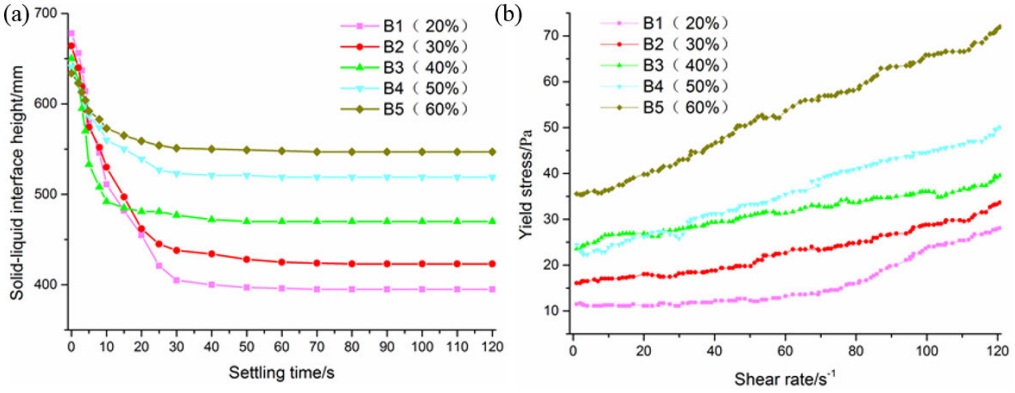

FIGURE 7. Group B sedimentation test results (a) Sedimentation monitoring and (b) Rheological characteristics.

of flocculant bridging has high strength, which is beneficial to the removal of free water in the structure. The surface chemistry of the flocculant not only affects the interaction between the flocculant and the tailings particles but also determines the surface properties of the flocs. The hydrophobic groups in the flocculant molecular structure, such as -CH_2- and -NH-, can facilitate the conversion of the adsorbed water to free water while reducing the viscosity of the underflow slurry, thereby improving the dewatering performance of the slurry.

The sedimentation result of A2 is good, and the yield strength of the underflow slurry is the lowest, which is conducive to further compaction and dehydration. A smaller yield stress is favourable for the stable operation of the thickener and the shearing effect of the flocs, while the sedimentation velocity and the underflow concentration are stable. The BASF high-molecular-weight cationic flocculant was chosen as the optimum flocculant for industrial applications. When the difference in sedimentation efficiency is small, the underflow fluidity test can be used as a supplementary indicator of the industrial sedimentation effect, and the result is remarkable. Therefore, the underflow rheological characteristics index was introduced to evaluate the practicality of the flocculation sedimentation.

B. EFFECT OF SOLID CONCENTRATION ON SEDIMENTATION BEHAVIOUR OF MPT

The sedimentation experiments with MPT sample was carried out at different solid concentrations (20%, 30%, 40%, 50%, and 60%) as Group B was the BASF high-molecular-weight cationic flocculant with a dosage of 20 g/t was used for the flocculation experiments. Based on the results of the previous tests, the main sedimentation behaviour of the MPT was completed in a short period of time. Therefore, the sedimentation data for the first 2 min was used as the basis for the analysis of Group B, and the sedimentation curve is shown in Figure 7(a). The underflow rheology characteristic tests of Group B were conducted to evaluate the sedimentation underflow quality, and the yield stress characteristic curves of each scheme are shown in Figure 7(b).

The test results showed that the yield stress of the MPT slurry increased linearly at a uniform rate of the rotational shear rate. The initial yield stress of the slurry ranged from 11.48 Pa to 35.57 Pa with different slurry solid mass concentrations. As the solid mass concentration of the tailings increased, the yield stress of the slurry underflow also gradually increased, indicating that the interparticle bonding was denser. When the slurry concentration was in the range of 40%-50%, the yield stress was relatively stable, and as the concentration continued to increase, the yield stress increased rapidly, which made the shear thinning of the slurry difficult.

It was observed from the comparison of different tailings treatment schemes that the overflow clarified faster when the solid mass concentration was low. When the solid mass concentration exceeded 30%, the supernatant liquid deposition rate decreased. The solid-liquid interface of each scheme was clearly visible in approximately 30 sec and then tended to be stable. Therefore, the interface height of this period was used to calculate the sedimentation velocity. The calculation formula is as follows:

$$v = \frac{H_0 - H_1}{t} \tag{1}$$

The solid processing capacity per unit area is usually used as a standard to measure the effect of flocculation and sedimentation:

$$G = \rho C_v v \times 10^{-2} \times 3600 \tag{2}$$

The calculation results of the parameters in Group B are shown in Table 4.

It can be seen from Figure 8(a) that the increase of the solid concentration caused a nearly linear decrease in the sedimentation velocity. The solid processing capacity per unit area first increased and then decreased, and the maximum appears at a concentration of 30%-50%. It can be seen from Figure 8(b) that both the yield stress and the viscosity increased with the solid mass concentration of the slurry. From the development of the yield stress and viscosity, when the slurry concentration was lower than 40%, the floc structure was easily destroyed, and the viscosity growth rate

TABLE 4. Test parameters of the MPT sedimentation in Group B.

Parameters	Solid mass concentration / (%)				
	20	30	40	50	60
Initial height / (mm)	678	664	650	641	634
Sedimentation time /($\cdot s^{-1}$)	30	30	30	30	30
Sedimentation height / (mm)	405	438	477	523	551
Sedimentation velocity / (mm $\cdot s^{-1}$)	9.10	7.50	5.76	3.90	2.80
Processing capacity per unit area / ($t \cdot h^{-1} \cdot m^{-2}$)	7.15	9.32	10.05	8.99	8.22

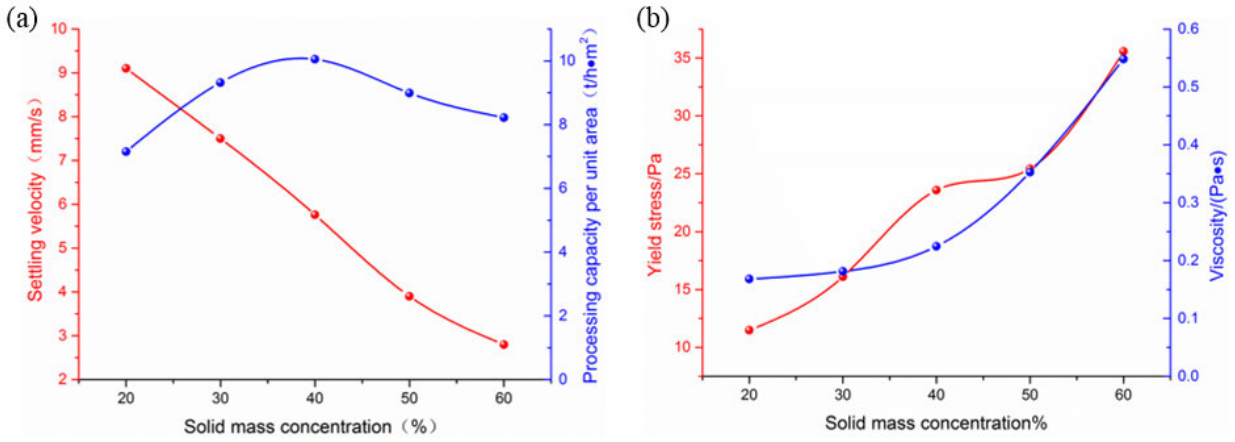

FIGURE 8. Group B sedimentation results (a) Sedimentation parameters (b) Rheological parameters.

was low. Although the slurry becomes gradually cloudy, the enclosed moisture and water in the flocs can be extruded to form free water inside the slurry structure, and the strength and distance of the flocs are within a suitable range. When the solid mass concentration of the slurry exceeded 40%, the interaction forces between the tailings particles increased, as does the yield stress and viscosity, which may cause the underflow to be consolidated. To control the flocculation dosage and the underflow quality of the MPT, the 40% slurry solid mass concentration scheme was choosen as the best choice.

C. EFFECT OF FLOCCULANT DOSAGE ON SEDIMENTATION BEHAVIOUR OF MPT

The sedimentation experiments with MPT were carried out as a function of flocculant dosages MPT slurries with different flocculant dosages (10 g/t, 15 g/t, 20 g/t, 25 g/t, and 30 g/t) as Group C. The solid concentration of the MPT slurry was 40%. The sedimentation data for the first 2 min was used as the basis for the analysis of Group C, and the sedimentation curve is shown in Figure 9(a). The underflow rheology characteristic tests of Group C were conducted to evaluate the sedimentation underflow quality, and the yield stress characteristic curves of each scheme are shown in Figure 9(b). The calculation results of the parameters in Group C are presented in Table 5. It can be seen from the sedimentation results that with the increase of the flocculant dosage, the influence range of the bridging effect expanded, and the sedimentation velocity and the treatment volume gradually increased. The maximum sedimentation velocity was 7. 4mm $\cdot$ s^{-1}, and the minimum velocity was 4. 57mm $\cdot$ s^{-1}. Based on the calculation result of Eq. 2, the maximum unit area processing amount calculated as 12.91t $\cdot$ h^{-1} $\cdot$ m^{-2}, and the minimum processing amount was 7.97t $\cdot$ h^{-1} $\cdot$ m^{-2}.

The test results are shown in Figure 10. The yield stress of the MPT slurry increased linearly at a uniform rate of rotational shear rate. The initial yield stress of the slurry ranged from 12.80 Pa to 28.47 Pa with different flocculant dosages. As the flocculant dosage increased, the yield stress of the slurry underflow also gradually increased, indicating that the interparticle bonding was denser. When the flocculant dosage was in the range of 15 g/t-25 g/t, the yield stress was relatively stable, and as the dosage continued to increase, the yield stress increased rapidly.

As the flocculant dosage increased, the sedimentation effect of the MPT slurry was enhanced, and the overflow was clearer. The yield stress and viscosity first increased and then decreased. When the flocculant dosage was 25 g/t, a low point was achieved with a yield stress of 20.22 Pa and a viscosity of 0.2043 Pa/s. When the flocculant dosage exceeded 25 g/t, the yield stress and viscosity of the slurry appeared to have a significantly accelerated growth trend. The main reason was that the excessive flocculant leads to an increase of adhesion between the flocs and had a certain influence on the surface properties of the tailings flocs, which intensified the compaction and dehydration process of the tailings. This phenomenon illustrates the influence mechanism of flocculant

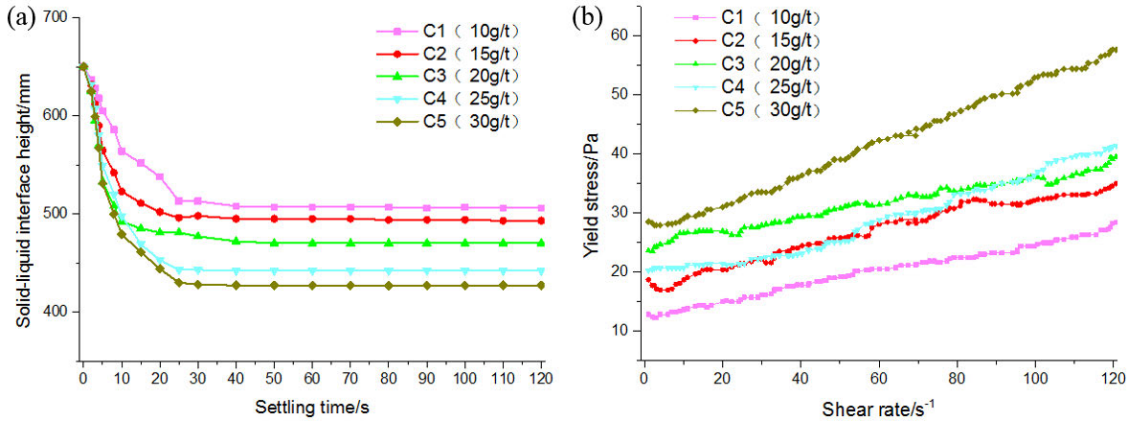

FIGURE 9. Group C sedimentation test results (a) Sedimentation monitoring and (b) Rheological characteristics.

TABLE 5. Test parameters of the MPT sedimentation in Group C.

Parameters	flocculant dosage / (g/t)				
	10	15	20	25	30
Initial height / (mm)	650	650	650	650	650
Sedimentation time / (s)	30	30	30	30	30
Sedimentation height / (mm)	513	498	477	443	428
Sedimentation velocity / (mm ·s^{-1})	4.57	5.06	5.76	6.90	7.40
Processing capacity per unit area / ($t \cdot h^{-1} \cdot m^{-2}$)	7.97	8.82	10.05	12.03	12.91

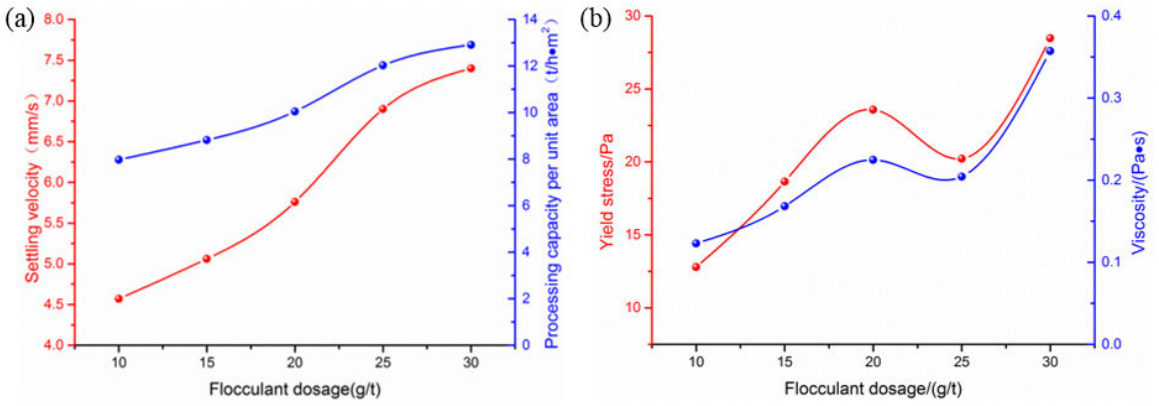

FIGURE 10. Group C sedimentation calculation results (a) Sedimentation parameters and (b) Rheological parameters.

consumption on the flocculation and sedimentation effect of the MPT. The sedimentation velocity and unit area treatment amount are positively correlated with the flocculant dosage in a certain interval. However, the flocculant treatment effect is negatively correlated with the flocculant dosage when excessive flocculant is added. Therefore, a flocculant dosage of 25 g/t was the best solution to guarantee the output and quality of the MPT underflow.

The concentration and rheological properties of the slurry change significantly under different flocculation and sedimentation conditions, which is consistent with the basic law of flocculation and dehydration. If the floc structure is irregular, slurries with a large yield stress and viscosity will be formed. This will cause strong adsorption of water by the flocs, which is difficult to compact and not conducive to the operation of the thickener. The MPT sedimentation process includes four parts: flocculation, sedimentation, compression and dehydration. The efficiency of the post-press dehydration process is related to the underflow concentration and the rheological characteristics. The experimental results show that an optimization method based on the rheological properties of the slurry can be used to optimize the flocculation sedimentation parameters of the MPT and can also be used as a reference and supplement for the conventional sedimentation test method. The combination of the two methods reflects the actual sedimentation effect and improves the reliability of the experimental conclusions.

D. MICROSCOPIC CHARACTERISTICS OF FLOCCULATION AND THE KINETIC MODEL

When the flocculant is added to the full tailings slurry, the following kinetic behaviour occurs:

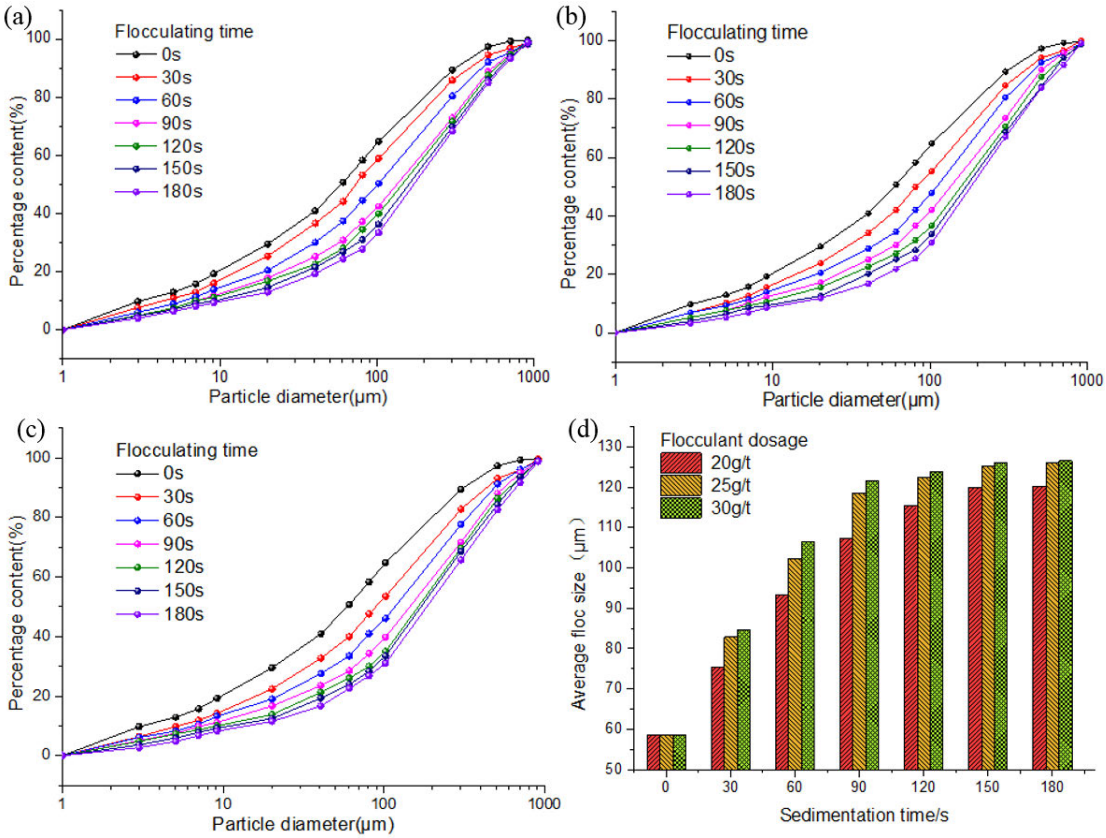

FIGURE 11. Microfloc formation characteristics with the different flocculant dosages (a) 20 g/t (b) 25 g/t (c) 30 g/t and (d) Average floc diameter growth.

1. The flocculant powder dissolves, hydrolyses, and finally mixes together in the flow field;

2. The bridging effect of the flocculant causes the particles to attract each other to form a preliminary flocculation phenomenon;

3. After the flocculant is absorbed by the tailings particles, an adsorption equilibrium structure is formed on the surface of the particles; and

4. The particles and the flocs approach and collide with each other and finally form flocs by electric neutralization and electric double layer compression along with a bridging effect.

Based on the results of the previous experiments, a microscopic verification test of the flocculation kinetics was performed. The experimental materials were an MPT slurry with a solid mass concentration of 40% and different dosages of flocculant (20 g/t, 25 g/t, and 30 g/t). The results are shown in Figure 11.

It can be concluded from Figure 11 that the particle size distribution curve gradually shifts to the right as the flocculation progresses; the floc size of the MPT particles continues to increase and eventually tends to be stable. The different flocculant dosage schemes are compared with reference to the average particle diameter. When the amount of flocculant is 20 g/t, the maximum average diameter is 120.21 μm. When the amount of flocculant is 25 g/t and 30 g/t, it is 126.13 μm and 120.53 μm, respectively. By analysing the test results, it can be concluded that the flocculation effect increases with the amount of flocculant but eventually tends to be saturated. This conclusion is basically consistent with the average particle diameter growth of the MPT and the results of the previous sedimentation tests. It can be seen from the comparison with the sedimentation test results that the particle size of the floc is still increasing when the solid-liquid interface in the slurry is relatively stable. Although slurry bleeding is rare during this period, flocculation and agglomeration still promote the growth of the MPT flocs, affecting the rheological properties of the slurry.

A particle size distribution provides the most intuitive results when determining the nature of the particles in the water and whether the flocculation method is effective. In essence, the flocculation method is specifically used to change the particle size distribution in the suspension, and sedimentation and filtration are only used to remove certain particles of a certain particle size. In this study, the floc growth gradient data was achieved by measuring the correlation of the particle size distribution as a function of time.

The main cause of floc formation is the interparticle force. During the flocculation and sedimentation process, the relative motion of water flow also causes collision and bridging among the particles. Particle agglomeration and destruction in the fluid bed occur almost simultaneously,

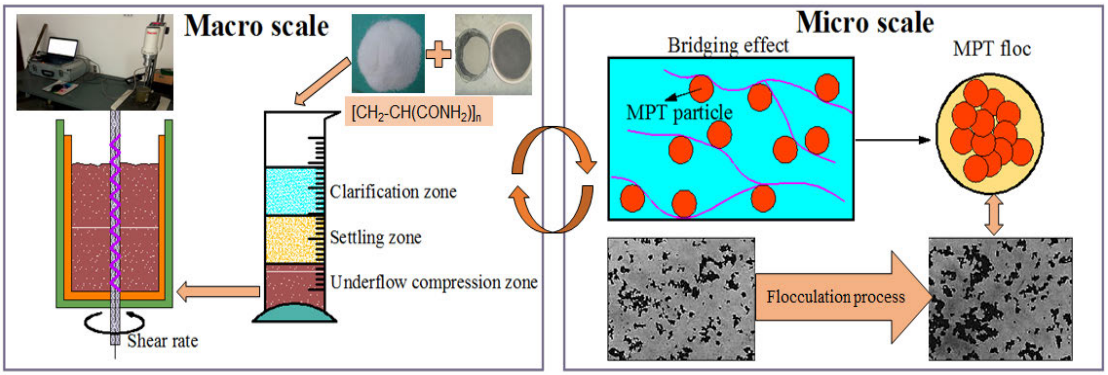

FIGURE 12. Description of the flocculation sedimentation test process.

exhibiting a dynamic equilibrium (Figure 12). When there is a hydrodynamically induced pressure difference, the shearing action and floc collision exceed the floc strength, and then floc destruction and particle separation will occur. The data obtained from the flocculation particle size test show that the flocculation process can be divided into three stages. The first stage is the initial flocculation stage, and the average diameter increases linearly with the settling time at this stage. The second stage is where the flocculation velocity gradually decreases. In the final stage of flocculation, the particle size in the system is basically unchanged, and the kinetic curve is horizontal. The reason for the flocculation velocity decrease in the later stages is generally considered to be due to a decrease in the number of particles, the collision frequency, and the collision efficiency as the flocs grow. In addition, the process of floc growth g is also affected by the impact of hydraulic stress.

There are a large number of suspended fine particles in the MPT slurry. With the occurrence of flocculation, the carbon-based and -NH2- groups on the polymer chain of the flocculant interact with the MPT particles through physical interactions. The heterogeneous ions in the MPT slurry produce two charged particles that attract each other under the influence of a free electric field to result in a surface flocculation phenomenon. From this point, the flocculation mechanism is the result of a combination of electric double layer compression and electrical neutralization. In fact, the backfilling slurry used in a stope is generally a sedimentation mortar under the influence of a polymer flocculant. After the polymer flocculant is hydrolysed and polycondensed, a linear polymer structure is formed, and the active group in the molecular chain is combined with the colloid through ionic bonds, hydrogen bonds, electrostatic attraction, etc. Many colloidal particles are adsorbed on the reactive groups, which make the particles larger and form flocs. The bridging effect has the greatest influence on the internal structural changes of the MPT slurry, whereas the formation of microscopic flocs has a significant effect on the sedimentation of the whole tailings. After which the formation of the flocs is finally reflected in the results of the macroscopic experiments. Therefore, it is necessary to analyse the dynamic characteristics of the floc formation process.

When Smoluchowski deduced the equation of floc dynamics, he believed that the collision of particles did not affect the motion of other particles, but that was not the case. That problem was later corrected by the water flow-induced collision efficiency correction factor α_T proposed by Mason [21]:

$$\frac{dN}{dt} = -\frac{16}{3}\alpha_T G r_0^3 N^2 \tag{3}$$

For the derivation of the flocculation kinetic equation, the mathematical model for solving this process is extremely complicated due to too many influencing factors, especially the dynamic process of using a flocculant due to the absorption and adsorption of particles on the surface. Other influencing factors, such as molecular remodelling and the relationship between the strength of the polymer segment and the hydraulic effect make the mathematical simulation and solution more complicated. The Brownian motion diffusion collision efficiency factor and the floc breaking factor by Liu [22] and Niu *et al.* [23], respectively, are introduced into Eq. 3.

$$\frac{dN}{\mathrm{d}t} = -\alpha_B \frac{4\mathrm{kT}}{3\mu} N^2 - \frac{16}{3}\alpha_T G r_0^3 N^2 + \beta_1 \frac{\tau_s}{\sigma_s}\left(\frac{\varepsilon}{\nu}\right)^{\frac{1}{2}} G d_B^2 N_B \tag{4}$$

In the initial stage of flocculation, small flocs are not easily damaged by hydraulics, and flocculation failure can be ignored. When the particles adsorbed with the polymer move, their collision radius increases. In the present study, the average primary particle size is relatively coarse, and the thickness of the polymer adsorption layer is negligible compared to the particle diameter. It is assumed that the step of adsorbing the polymer on the surface of the particles is a fast step, and the flocculation process is carried out by the collision between particles adsorbing the polymer. When the average size of the particles is greater than 1 μm, the influence of the first Brownian diffusion can be ignored, and the volume fraction of the particles at the initial stage of flocculation

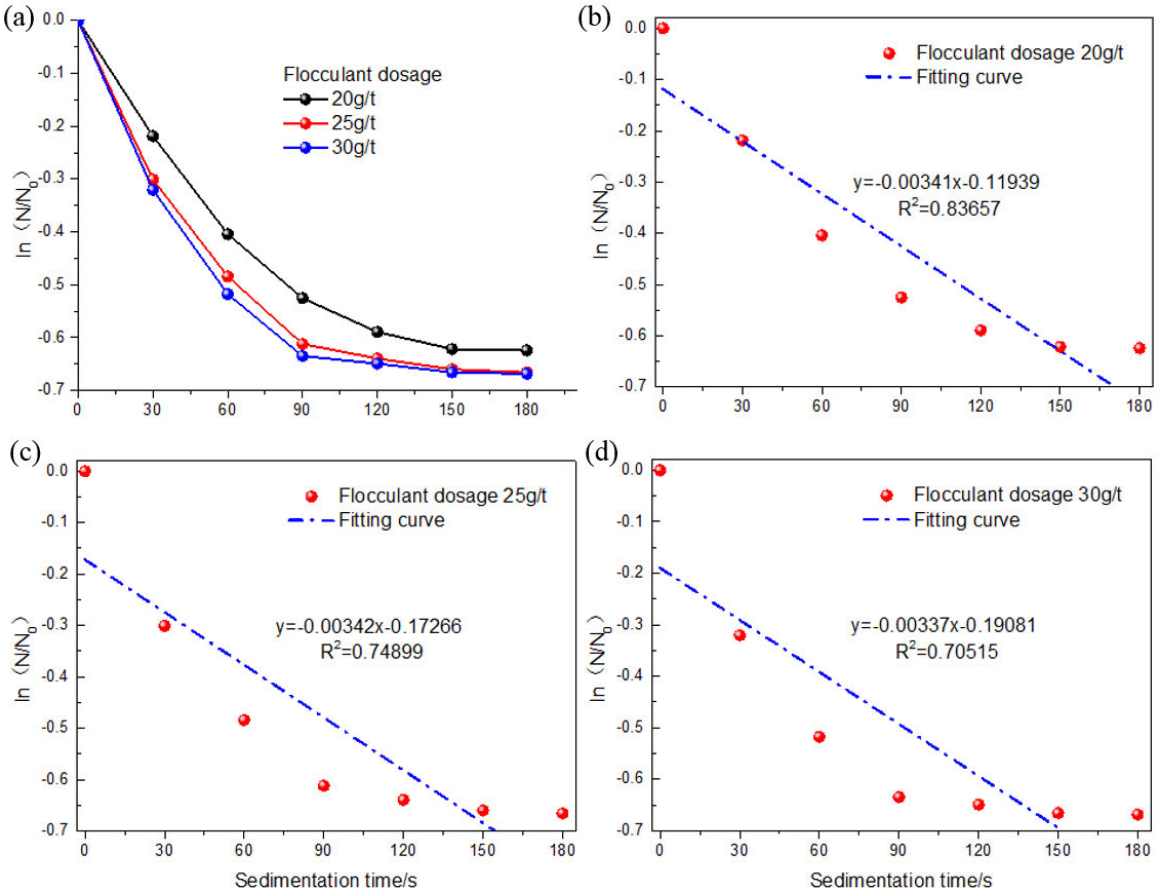

FIGURE 13. Time-varying state of mass at different flocculant dosages: (a) Monitoring data (b) 20 g/t (c) 25 g/t and (d) 30 g/t.

can be approximated as a constant (φ_0). Introduction of the correction factor ω allows the following to be concluded:

$$\varphi_0 = -\frac{4\pi}{3}\omega r^3 N \tag{5}$$

According to the initial boundary conditions of flocculation, when t = 0, $N = N_0$, and Eq. 5 is integrated, the relationship between the total floc density and time is as follows:

$$ln\frac{N}{N_0} = -\frac{4\varphi_0\alpha_T G}{\pi\omega}t = -kt \tag{6}$$

$$N_0 = -\frac{3C}{4\pi r_0^3\rho_0} \tag{7}$$

$$N = -\frac{3C}{4\pi r_i^3\rho_i} \tag{8}$$

According to the stokes sedimentation equation:

$$V_s = \sqrt{\frac{4g\rho_e d}{3C_D\rho_w}} \tag{9}$$

The relationship between $ln(N/N_0)$ and time can be obtained by combining Eq. 6 with Eq. 9, as shown in Figure 13(a). It can be concluded from the figure that the absolute value of $ln(N/N_0)$ increases with the occurrence of the flocculation process, but the growth trend gradually becomes slower. From the comparison of the scheme curves with a flocculant dosage of 25 g/t and 30 g/t, it can be concluded that when the flocculation dosage exceeds a certain level, the flocculant effect will decrease. This phenomenon is due to the fact that in the flow field of MPT particles, the contact area between the flocculant and the particles is saturated, and the bridging effect is limited. The increase of the polymer flocculant will occupy the space in the flow field and reduce the flocculation range. The flocculation sedimentation scheme at different dosages was fitted according to Eq. 6, and the results are shown in Figure 13.

As shown in Figure 13, the different flocculation dosage regimes have different settling constants. As the agitation velocity increases, the initial rate constant of floc growth also increases. When the dosage of the drug reaches a certain level, the initial rate constant slowly changes. The concentration of fine particles is a complex process. In previous studies in this article, the effect of changes in the particle volume fraction and flow shear force on floc size was not fully considered. To be precise, the above kinetic equations are only applicable to the description of the very short process at which flocculation occurs. As the flocculation continues to increase, the number of particles in the entire system decreases, and the reduction in the collision frequency between particles will have an effect on the dynamic characteristics. It can be

seen from the function fitting results that the sedimentation velocity drops sharply after a certain period of sedimentation, and the particle size variation characteristics are no longer obvious, resulting in a poor fitting effect. The slope of the fitted curve also does not match the results of the macroscopic test.

The microscopic flocculation kinetic research system involves a complex dispersion medium, polymer surface adsorption, polymer remodelling after adsorption, and the strength and hydraulics of the polymer segments, which leads to some uncertain parameters. However, a simple and effective description of the test process kinetic curve is still necessary. Under constant settling conditions, the kinetic equation can be described as follows: [24]–[26]

$$\frac{dN_A}{\mathrm{dt}} = -A_1 N_A^2 + A_2 N_B \tag{10}$$

where A_1 and A_2 are defined as the velocity constants of flocculation and fragmentation, respectively. To change the inaccuracy of a single variable system description method, in many flocculation kinetic studies the flocs are divided into large and small flocs that change synchronously. N_A and N_B are defined as the quantitative concentration of large flocs and small flocs, respectively. In the theory proposed by Dickinson et al. [27], d_A and d_B are defined as a set of synergistic variables, such as the characterization of the particle size of the large and small flocs, respectively. On this basis, the following assumptions are made:

(1). In each small floc with particle size d_A, the number of particles with the original particle size d_0 is $n_A = \left(\frac{d_A}{d_0}\right)^{D_F}$;

(2). In each large floc with particle size d_B, the number of small flocs with particle size d_A is $n_B = \left(\frac{d_B}{d_A}\right)^{D_F}$;

(3). The initial small floc group integral number is unchanged, and the large floc group is consistent with the formation mechanism of the small floc group;

(4). In each large floc with particle size d_B, the number of particles with original particle size d_0 is $n_B = \left(\frac{d_A}{d_0}\right)^{D_F}\left(\frac{d_B}{d_A}\right)^{D_F}$, and D_F is the average fractal dimension of the floc.

The fractal dimension of flocs is generally considered to belong to a non-Euclidean system, so the calculation result is less than 3. For the microscopic imaging of flocs, it is necessary to analyse the morphology from the perspective of dimensionality. Therefore, the Gangepain method was adopted. Fractal dimensions can be obtained by taking the image as a three-dimensional surface and then calculating the number of boxes covered [28], [29]. The steps of this method are as follows:

(1) For an image, MxM can be considered a surface in three-dimensional space. The length is M, the width is M, and the height is L, where L is the pixel level of the image.

(2) Divide the plane (MxM) into a grid of RxR size and divide the coordinates of "height" in the same way, but the unit of division is RxL/M. In this way, the three-dimensional space in which the image is located is divided into many "boxes", and the number of divisions in the three-dimensional direction is guaranteed to be uniform.

(3) In each of the divided grids, we find the maximum pixel value u and the minimum pixel value b for continuous iteration and finally calculate the number of boxes that can cover the area. The number of boxes is recorded as n(i,j)—assuming the current (i, j) of the grid—then n(i,j) = [(u-b+R-1)/R] (Round the number).

(4) Sum the number of boxes per RxR and record it as N, so now, N = sum(n(i,j)).

(5) At this point, the theoretical fractal dimension D_F = -logN/logR, when R tends to infinity. In reality, R is a finite value, so a set of N can be found by changing the value of R. Under linear fitting conditions, the slope of the resulting line is D_F.

To study the floc growth system and dynamic characteristics, the above fractal dimension algorithm was compiled by UDF in MATLAB software, and the fractal dimension calculation model was compiled. The main part of the compiled content is as follows:

```
for row = 1:blockSizeR:M
for col = 1:blockSizeC:M
row1 = row;
row2 = row1 + blockSizeR - 1;
col1 = col;
col2 = col1 + blockSizeC - 1;
%extract block
oneBlock = im(row1:row2,col1:col2);
maxI = max(max(oneBlock));
minI = min(min(oneBlock));
%number of boxes
nb = ceil((double(maxI)-double(minI)+1)/ ld);
...
subplot(3, 1, 2);
N = log(Nr)./log(2);
S = log(scale)./log(2);
p = polyfit(S, N, 1);
f = polyval(p, S);
fprintf('Dimension = %d\n',p(1));
plot(S,N,'o–',S,f,'*–');
...
for j = 1:length(N)
x = (((m * S(j)) + c) - N(j))/(1 + (m * m));
if x < 0
```

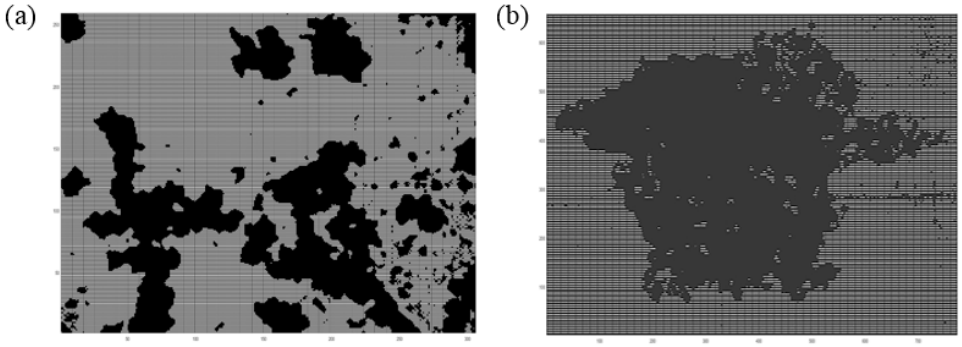

FIGURE 14. Pixelized microscopic floc morphology: (a) 1 mm and (b) 10 μm.

```
y = y + x * −1;
    else
y = y + x;
    end
    end
n = length(N);
E = (1/n)*sqrt(y);fprintf('Error = %d\n',E);
```

The microscopic floc image is pixelated and imported into the model for calculation, as shown in Figure 14. According to the calculation results of the model, the fractal dimension of Figure 15(b) is 2.26 with an error of 5%.

According to the principle of total particle balance, the initial number of particles in the flow field is:

$$N_0 = N_A \left(\frac{d_A}{d_0}\right)^{D_F} + N_B \left(\frac{d_A}{d_0}\right)^{D_F} \left(\frac{d_B}{d_A}\right)^{D_F} \tag{11}$$

At time t, the total number of particles is:

$$N = N_A + N_B \tag{12}$$

It can be deduced after the above two equations are combined:

$$N_B = \left[N_0 - N_A \left(\frac{d_A}{d_0}\right)^{D_F}\right] / \left(\frac{d_B}{d_0}\right)^{D_F} \tag{13}$$

Substituting Eq. 13 into Eq. 10, it can be described as follows:

$$\frac{dN_A}{\mathrm{dt}} = -A_1 N_A^2 - A_2 N_A \left(\frac{d_A}{d_B}\right)^{D_F} + A_2 N_0 \left(\frac{d_0}{d_B}\right)^{D_F} \tag{14}$$

For Eq. 14, let: $\mathrm{a} = -A_2 N_0 \left(\frac{d_0}{d_B}\right)^{D_F}$, $\mathrm{b} = -A_2 \left(\frac{d_A}{d_B}\right)^{D_F}$, $\mathrm{c} = A_1$, and integrate on this basis:

$$\frac{1}{\left(b^2 - 4ac\right)^{1/2}} ln \times \frac{\left(2cN_A + b - \sqrt{b^2 - 4ac}\right)\left(2cN_0 + b + \sqrt{b^2 - 4ac}\right)}{\left(2cN_A + b + \sqrt{b^2 - 4ac}\right)\left(2cN_0 + b - \sqrt{b^2 - 4ac}\right)} = -t \tag{15}$$

Substituting the values of a, b, c and N_A into Eq. 15, it can be deduced that:

$$ln\frac{N}{N_0} = -\left[A_2^2 \left(\frac{d_A}{d_B}\right)^{2D_F} + 4A_1 A_2 N_0 \left(\frac{d_0}{d_B}\right)^{D_F}\right]^{1/2} t - \Delta \tag{16}$$

In Eq. 16, Δ can be used as a modulation function. Due to the synchronous formation mechanism of large flocs and small flocs in the initial stage of flocculation, $\frac{d_A}{d_B} = \frac{d_0}{d_A}$. By replacing d_A with the average particle size d, Eq. 16 can be simplified as follows:

$$d^{D_F} ln\frac{N}{N_0} = -A_3 t - \Delta_1 \tag{17}$$

In Eq. 17, $A_3 = d_0^{D_F}\left(A_2^2 + 4A_1A_2N_0\right)^{1/2}$, so that $d^{D_F} ln\left(N/N_0\right)$ can be used as a dependent variable to make a linear relationship with time t, which can then describe the concentrated sedimentation process and optimizes the kinetic equation for a longer time interval. The fitting results are shown in Figure 15. It can be concluded from the figure that the value of A_3 ranges from -5.568×10^{-5} to -6.280×10^{-5} under different dosages. This change is good proof of the sedimentation efficiency results of the different flocculation dosages in the macroscopic experiments. From the comparison of the fitting effects, the evaluation method using $d^{D_F} ln\left(N/N_0\right)$ as the dependent variable is more in line with the formation of the flocs in the experiment.

According to the research results of Mason and Kusters et al. [30]–[32], the floc impact efficiency decreases as the D_F power of the particle size increases. Therefore, Eq. 6 can be transformed into:

$$ln\frac{N}{N_0} = -\frac{4\varphi_0 G}{\pi \mathrm{k} d^{D_F} \omega}\mathrm{t} = -\frac{k_1}{d^{D_F}} t \tag{18}$$

and a slope result similar to that of Eq. 17 is obtained, which also confirms the usability of Eq. 17. The sedimentation velocity is positively correlated with the flocculant dosage over a certain interval. However, the flocculant treatment effect is negatively correlated with the flocculant dosage when excessive flocculant is added. The value of A_3 under different flocculant dosages is a good proof of this conclusion. This model is able to describe the kinetic characteristics

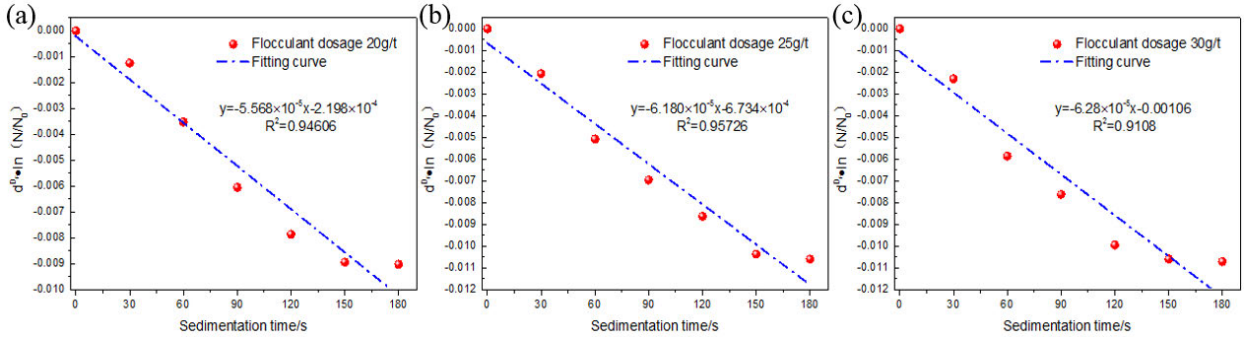

FIGURE 15. Fitting results of $d^{D_F} ln\,(N/N_0)$ under different flocculant dosages: (a) 20 g/t (b) 25 g/t and (c) 30 g/t.

of the particle agglomeration velocity before equilibrium. The N value in the formula is the total number of particles per unit volume at different times and reflects the influence of flocculation destruction in the system.

IV. CONCLUSION

Based on MPT particle material property tests, agglomeration characteristics and sedimentation principles, MPT flocculation sedimentation chamber experiments were carried out to study the concentration and sedimentation behaviour of MPT under different flocculant types, initial slurry concentrations and dosages. The concentrated underflow rheological shear test was carried out to analyse the actual effect under different flocculation and sedimentation conditions from the underflow quality observations. The results of the preliminary test and the variation test of the particle size characteristic of the whole tailings were combined with the floc equilibrium equation, and a behaviour equation corresponding to the microscopic dynamics of the flocs was established. Subsequently, the reliability of the macroscopic test parameters was verified by microscopic analysis. The optimized parameters were tested using the existing industrial backfilling system of the Gaofeng Mine, and the test results were satisfactory. The main conclusions of the experiments and research in this paper are as follows:

(1) The amount of MPT and the control of the flocculant has an effect on floc bridging. In the MPT solid mass concentration experiment, if the solid mass concentration is too low, the production efficiency cannot meet the industrial demand, even though the processing velocity is fast. If the solid mass concentration is too high, the flow field force is enhanced, which is not conducive to the later MPT dehydration, and the consumption of the settling materials is large.

In the flocculant dosage experiment, when the flocculant dosage is low, the sedimentation rate is slow; when the flocculant dosage is too high, the yield stress and viscosity of the slurry are easily increased, and the sedimentation efficiency is gradually reduced.

(2) In the flocculation sedimentation test, it can be visually seen that the sedimentation velocity is very fast, and the total amount of slurry in the sedimentation process is relatively stable. The amount of cleaned water is constantly increasing, and the amount of slurry is continuously reduced during the process. The solid mass concentration of the MPT and the flocculant dosage has an obvious influence on the formation of the flocs, which affects the yield stress and viscosity of the slurry. The optimum results of the indoor test were achieved with BASF high-molecular-weight cationic flocculant at a dosage of 25 g/t, which results in an MPT slurry with a solid mass concentration of 40%. In this scheme, the yield stress and viscosity of the slurry are suitable, and the quality of the bottom flow of the slurry after sedimentation is good, which is beneficial for controlling the knot phenomenon in the concentrated underflow.

(3) From the rheological characteristics of the concentrated underflow experiment, it can be concluded that the flocculation sedimentation effect is directly related to the rheological characteristics of the underflow, and the compression operation is affected by the rheological properties of the MPT slurry. Combined with the flocculation sedimentation experiment, the flocculation sedimentation parameters of the tailings were optimized according to the rheological properties of the slurry, and the shear failure and compaction dewatering performance of the flocs were evaluated by the yield stress and viscosity as standards. This evaluation standard is beneficial to the stable operation of the thickener and the underflow quality. This comprehensive experimental evaluation method facilitates the precise optimization of flocculation sedimentation parameters as well as industrial applications.

(4) The growth of the floc follows microscopic flocculation kinetics, and the growth rate of the floc is directly related to the particle size of the floc. The flocculation sedimentation particle size characteristic test experiment was carried out with different flocculant dosages. To increase the application range of the kinetic equation and the accuracy of the characteristic variables, the fractal dimension D_F of the floc size is introduced, and the condensed kinetic characteristic equation describing the flocculation and sedimentation effect at the initial stage of flocculation is obtained. It can be seen from the test results with different flocculant dosages that the flocculation effect increases with the amount of flocculant, but the effect will gradually reach saturation, which is consistent with the macroscopic sedimentation experiment results.

ACKNOWLEDGMENT

For the contribution of the author to this article: Keping Zhou and Rugao Gao conceived and designed the experiments; Qifan Ren and Rugao Gao performed the experiments; Jian Zhang and Hongquan Guo analyzed the data; Rugao Gao wrote the paper."

NOMENCLATURE

H_0 = initial liquid level height [mm]
t = sedimentation time [s]
ρ = density [kg/m^3]
T = absolute temperature [K]
N = particle concentration [cm^{-3}]
G_0 = velocity gradient [-]
β_1 = floc fracture constant [-]
σ_s = floc strength [Pa]
N_B = large floc content [cm^{-3}]
C = weight concentration [%]
V_s = floc sedimentation velocity [m/s]
ρ_e = floc effective density [kg/m^3]
H_1 = solid-liquid interface height [mm]
G = solid processing capacity per unit area [$t \cdot h^{-1} \cdot m^{-2}$]
α_B = collision efficiency factor [-]
μ = hydrodynamic viscosity [$Pa \bullet s$]
α_T = collision correction factor [-]
r_0 = initial particle size [μm]
τ_s = shear stress [N/cm^2]
d_B = large floc size [μm]
N_0 = primary particle concentration [cm^{-3}]
r_i = particle size at a certain time [μm]
C_D = resistance coefficient [-]
ρ_w = water density [kg/m^3]

REFERENCES

[1] E. Asensio, C. Medina, M. Frías, M. Isabel, and S. de Rojas, "Characterization of ceramic-based construction and demolition waste: Use as Pozzolan in cements," *J. Amer. Ceram. Soc.*, vol. 99, no. 12, pp. 4121–4127, 2016. doi: 10.1111/jace.14437.
[2] T. Belem and M. Benzaazoua, "Design and application of underground mine paste backfill technology," *Geotech. Geolog. Eng.*, vol. 26, pp. 147–174, Apr. 2008. doi: 10.1007/s10706-007-9154-3.
[3] Amjad Tariq and E. K. Yanful, "A review of binders used in cemented paste tailings for underground and surface disposal practices," *J. Environ. Manage.*, vol. 131, pp. 138–149, Dec. 2013. doi: 10.1016/j.jenvman.2013.09.039.
[4] Q. Chen, Q. Zhang, C. Qi, A. Fourie, and C. Xiao, "Recycling phosphogypsum and construction demolition waste for cemented paste backfill and its environmental impact," *J. Clean. Prod.*, vol. 186, pp. 418–429, Jun. 2018.
[5] C. Qi, A. Fourie, Q. Chen, X. Tang, Q. Zhang, and R. Gao, "Data-driven modelling of the flocculation process on mineral processing tailings treatment," *J. Cleaner Prod.*, vol. 196, pp. 505–516, Sep. 2018.
[6] D. M. McHaina, S. Januszewski, and R. L. Hallam, "Development of an environmental impact and mitigation assessment program for a tailings storage facility stability upgrade," *Int. J. Surf. Mining, Reclamation Environ.*, vol. 15, no. 2, pp. 123–140, 2001. doi: 10.1076/ijsm.15.2.123.3415.
[7] B. J. Burd, "Evaluation of mine tailings effects on a benthic marine infaunal community over 29 years," *Mar. Environ. Res.*, vol. 53, no. 5, pp. 481–519, Jun. 2002. doi: 10.1016/S0141-1136(02)00092-2.
[8] E. V. Derekv, "A Review of Some Environmental Issues Affecting Marine Mining," *Mar. Georesources Geotechnol.*, vol. 19, no. 1, pp. 51–63, 2001. doi: 10.1080/10641190109353804.
[9] H. Z. H. J. Jiao Wang, "Rule and mechanism of flocculation sedimentation of unclassified tailings," *J. Univ. Sci. Technol. Beijing*, vol. 32, pp. 702–707, Jun. 2010.
[10] S. Li, X. M. Wang, and Q. L. Zhang, "Dynamic experiments on flocculation and sedimentation of argillized ultrafine tailings using fly-ash-based magnetic coagulant," *Trans. Nonferrous Met. Soc. China* vol. 26, no. 7, pp. 1975–1984, Jul. 2016. doi: 10.1016/S1003-6326(16)64308-X.
[11] A. T. Owen, T. V. Nguyen, and P. D. Fawell, "The effect of flocculant solution transport and addition conditions on feedwell performance in gravity thickeners," *Int. J. Mineral Process.*, vol. 93, no. 2, pp. 115–127, Oct. 2009. doi: 10.1016/j.minpro.2009.07.001.
[12] S. Li and X.-M. Wang, "Fly-ash-based magnetic coagulant for rapid sedimentation of electronegative slimes and ultrafine tailings," *Powder Technol.*, vol. 303, pp. 20–26, Dec. 2016. doi: 10.1016/j.powtec.2016.09.016.
[13] Y. Q. Zhao and D. H. Bache, "Conditioning of alum sludge with polymer and gypsum," *Colloids Surf. A, Physicochem. Eng. Aspects*, vol. 194, nos. 1–3, pp. 213–220, Dec. 2001. doi: 10.1016/S0927-7757(01)00788-9.
[14] C. P. Chu and D. J. Lee, "Moisture distribution in sludge: Effects of polymer conditioning," *J. Environ. Eng.*, vol. 125, no. 4, pp. 340–345, Apr. 1999. doi: 10.1061/(ASCE)0733-9372(1999)125:4(340).
[15] H. Wang, H. Deng, L. Ma, and L. Ge, "The effect of carbon source on extracellular polymeric substances production and its influence on sludge floc properties," *J. Chem. Technol. Biotechnol.*, vol. 89, no. 4, pp. 516–521, Apr. 2014. doi: 10.1002/jctb.4147.
[16] X. Wang, J. Liu, and Q. Chen, "Optimal flocculating sedimentation parameters of unclassified tailings," *Sci. Technol. Rev.*, vol. 32, no. 17, pp. 23–28, 2014.
[17] K. Y. Yeap, J. Addai-Mensah, and D. A. Beattie, "The pivotal role of polymer adsorption and flocculation conditions on dewaterability of talcaceous dispersions," *Chem. Eng. J.* vol. 162, no. 2, pp. 457–465, Aug. 2010. doi: 10.1016/j.cej.2010.04.021.
[18] L. Spinosa, A. Ayol, J. C. Baudez, R. Canziani, P. Jenicek, A. Leonard, W. Rulkens, G. Xu, and L. Van Dijk, "Sustainable and innovative solutions for sewage sludge management," *Water*, vol. 3, no. 2, pp. 702–717, 2011. doi: 10.3390/w3020702.
[19] Y. Xiao, Y. Tu, Y. Ren, and Z. Xu, "Optimization of packing state in brown coal water slurry based on the two-grade fractal model," *Fuel*, vol. 168, pp. 54–60, Mar. 2016. doi: 10.1016/j.fuel.2015.11.078.
[20] T. Belem and M. Benzaazoua, "Predictive models for prefeasibility cemented paste backfill mix design," in *Proc. 3rd Int. Conf. Post-Mining*, Feb. 2008, pp. 6–8.
[21] E. Dickinson and S. R. Euston, "Short-range structure of simulated flocs of particles with bridging polymer," *Colloids Surf.*, vol. 62, no. 3, pp. 230–232, Feb. 1992. doi: 10.1016/0166-6622(92)80005-M.
[22] L. Heng, "The study of flocculation of fine phosphate ore residues in leaching solutio," Ph.D. dissertation, Sichuan Univ, Chengdu, China, 2000.
[23] X. Niu, S. Li, and L. Zhang, "Study on flocculation kinetics of fine hematite in stirring flow field," *Conserv. Util. Miner Resour.*, vol. 5, pp. 58–63, 2017.
[24] S. Lu, Y. Ding, and J. Guo, "Kinetics of fine particle aggregation in turbulence," *Adv. Colloid Interface Sci.*, vol. 78, no. 3, pp. 197–235, Nov. 1998. doi: 10.1016/S0001-8686(98)00062-1.
[25] S. Lu and J. Guo, "Kinetics of coagulation of fine mineral particles in a stirred tank," *Colloids Surf. A, Physicochem. Eng. Aspects*, vol. 84, nos. 2–3, pp. 195–205, May 1994. doi: 10.1016/0927-7757(93)02657-z.
[26] J. Ren, S. Lu, J. Shen, and C. Yu, "Research on the composite dispersion of ultra fine powder in the air," *Mater. Chem. Phys.*, vol. 69, nos. 1–3, pp. 204–209, Mar. 2001. doi: 10.1016/S0254-0584(00)00396-5.
[27] H. Liu and B. H. Zhong, "Flocculation of fine phosphate ore residues in leaching solution—The study of floc structure," *J. Chem. Eng. Chin. Universities*, vol. 15, no. 2, pp. 138–143, 2001.
[28] M. Long and F. Peng, "A box-counting method with adaptable box height for measuring the fractal feature of images," *Radioengineering*, vol. 22, no. 1, pp. 208–213, Apr. 2013.
[29] B. Stark, M. Adams, D. H. Hathaway, and M. J. Hagyard, "Evaluation of two fractal methods for magnetogram image analysis," *Sol. Phys.*, vol. 174, nos. 1–2, pp. 297–309, Aug. 1997. doi: 10.1023/a:1004908523578.
[30] K. A. Kusters, J. G. Wijers, and D. Thoenes, "Aggregation kinetics of small particles in agitated vessels," *Chem. Eng. Sci.*, vol. 52, no. 1, pp. 107–121, Jan. 1997. doi: 10.1016/S0009-2509(96)00375-2.

[31] F. Baldassarre, M. Cacciola, and G. Ciccarella, "A predictive model of iron oxide nanoparticles flocculation tuning Z-potential in aqueous environment for biological application," *J. Nanopart. Res.*, vol. 17, p. 377, Sep. 2015. doi: 10.1007/s11051-015-3163-6.

[32] P. A. Arp and S. G. Mason, "Orthokinetic collisions of hard spheres in simple shear flow," *Can. J. Chem.*, vol. 54, no. 23, pp. 3769–3774, 1976. doi: 10.1139/v76-541.

RUGAO GAO (M'18) received the Ph.D. degree in mining engineering from Central South University, Changsha, China, in 2018. He is currently the Assistant Director of the Research Center for Mining Engineering and Technology in Cold Regions, Central South University. He is also the Chief Researcher with the Key Technology Research for Super Large-Scale Mining Process Cooperation Project, State Administration of Work Safety. His research interests include computational mechanics, numerical simulation, and industrial applications of multiphase flow theory.

KEPING ZHOU received the Ph.D. degree in mining engineering from Central South University, Changsha, China, in 2000, where he was the Dean of the School of Resources and Safety Engineering. His positions and honorable titles, include the New Century Excellent Talents in University of Ministry of Education of China, an Academic Leader in Hunan, the Commissioner of the Mining Committee, the Nonferrous Metals Society of China, the Vice Chairman of the Intelligent Information Commission of the Nonferrous Metals Society of China, and the Commissioner of Academic Committee on Safety and Equipment of Metal Mines of China. His research interests include continuous mining technology and equipment in deep metal mine, theoretical method, and the application of mining environment regenerating. He was a recipient of the First Class Prizes in Science and Technology Award of China Nonferrous Metal Industry Association.

JIAN ZHANG (M'18) was born in Changsha, Hunan, China, in 1988. He received the B.S. and M.S. degrees in mining engineering from Central South University. He is currently pursuing the Ph.D. degrees in rock mechanics with the School of Resources and Safety Engineering, Central South University, and also with The University of Adelaide. His research interests include rock mechanics and mining methods.

HONGQUAN GUO received the Ph.D. degree in mining engineering from Central South University. He has been a Visiting Scholar in civil engineering with Federation University Australia for two years. His research interests include computational mechanics, rock mechanics, and numerical methods.

QIFAN REN received the M.S. degree in mineral engineering from Central South University, Changsha, China, in 2019. He is currently pursuing the Ph.D. degree in civil engineering with the University of Lisbon. His research interests include solid waste disposal and finite element numerical simulation.